Engineering Science and Technology, an International Journal xxx (2017) xxx–xxx

HOSTED BY

ELSEVIER

Contents lists available at ScienceDirect

Engineering Science and Technology, an International Journal

journal homepage: www.elsevier.com/locate/jestch

Review

GMAW dissimilar welding of AISI 409 ferritic stainless steel to AISI 316L austenitic stainless steel by using AISI 308 filler wire

Nabendu Ghosh *, Pradip Kumar Pal, Goutam Nandi

Mechanical Engineering Department, Jadavpur University, Kolkata 700032, WB, India

ARTICLE INFO

Article history:
Received 24 September 2016
Revised 26 March 2017
Accepted 3 August 2017
Available online xxxx

Keywords:
MIG welding
Taguchi desirability analyses
Tensile test
Optimization

ABSTRACT

To study and analyze the effects of welding parameters: welding current, gas flow rate and nozzle to plate distance, on ultimate tensile strength (UTS) and Yield Strength (YS) in MIG welding of AISI409 ferritic stainless steel to AISI 316L Austenitic Stainless Steel materials. Experiments have been conducted as per L9 orthogonal array of Taguchi method. The observed data of UTS and YS have been interpreted, discussed and analyzed with use of Taguchi Desirability analyses.

Contents

1. Introduction

Dissimilar metal joints are used in various engineering applications such as nuclear power plant, coal fired boilers, automobile manufacturing industry etc. Very often joining of dissimilar metals utilizes pressure welding instead of other joining methods [1]. Dissimilar welding is the joining between two different materials by any welding process. Joining of dissimilar materials may significantly reduce the weight of product and minimize the cost production as well, without compromising the safety and structural requirements. Dissimilar weld must possess sufficient tensile strength and ductility, so that the joint will not fail within the weld. Dissimilar metal joints are used in various engineering

* Corresponding author.
E-mail addresses: nabendu2003_ghosh@yahoo.co.in (N. Ghosh), pradippal54@yahoo.com (P.K. Pal), gnandi87@gmail.com (G. Nandi).

Peer review under responsibility of Karabuk University.

http://dx.doi.org/10.1016/j.jestch.2017.08.002
2215-0986/

applications such as nuclear power plants, coal fired boilers, automobile manufacturing industry [1] etc. Dissimilar materials have been joined by different welding operations which include gas metal arc welding (GMAW), gas tungsten arc welding (GTAW), submerged arc welding (SAW), fusion welding, pressure welding, explosion welding, friction welding [2], diffusion welding, brazing, and soldering [3]. Among the other welding processes GMAW is a versatile process which is extensively used in manufacturing of variety of ferrous and non-ferrous metals as it greatly improves the quality characteristics of the weldment [4].

Gas metal arc welding (GMAW) is an arc welding process in which the source of heat is an arc formed between consumable metal electrode and the work piece with an externally supplied gaseous shield of gas either inert such as argon and /or helium [5]. Weld quality mainly depends on features of bead geometry, mechanical-metallurgical characteristics of the weld as well as on various aspects of weld chemistry, and these features are expected to be greatly influenced by various variables such as welding geometry, groove angle, shielding type and mixture [4], and different input parameters: current, voltage, electrode stick-out, gas flow rate, edge preparation, position of welding, welding speed, nozzle to plate distance[6,7], etc. Moreover, the cumulative effect of various input parameters determines the extent of joint strength that should meet the functional aspects of the weld in practical field of application [8]. Therefore, preparation of a good quality weld seems to be a challenging job. Dissimilar metal combination between ferritic stainless steels and austenitic stainless steels (F/A) is in demand in certain applications, and, for example, it is commonly employed in $TiCl_4$ reduction retorts, because austenitic stainless steel has good creep strength and oxidation resistance which are required in the higher temperature regions, while ferritic stainless steel is preferred to avoid the problem of nickel leaching by molten magnesium [2].

Type AISI 316 austenitic stainless steels are widely used in many industrial applications due to its excellent corrosion resistance, fabricability, and they possess good mechanical properties at elevated temperatures [9,10], and their availability in the market with cheaper cost [11] has make them popular. Typical uses of 316 stainless steels include steam generating plants as piping and super heater material [9]. The stainless steel (SS) 316L is a chromium-nickel-molybdenum austenitic stainless steel developed to provide improved corrosion resistance to SS 304/304L in moderately corrosive environments. Type 316L is an extra-low carbon version of Type 316 that minimizes harmful carbide precipitation due to welding. The addition of molybdenum improves general corrosion and chloride pitting resistance [12–14]. The material austenitic stainless steels 316L is selected because the material contains low carbon and it has a good weldability factor [9]. Austenitic stainless steel (ASS) such as type 316L is usually preferred over other austenitic varieties as a structural material due to its higher corrosion resistance and superior mechanical properties both at low and high temperatures.

Ferritic stainless steels (FSS) have body centered cubic crystal [15] are less ductile than austenitic steel, and are not hardenable by heat treatment like martensitic steels. Older ferritics (i.e. AISI 430) are used mainly for household utensils and other applications not demanding in excellent anti-corrosion properties. They are the second largest selling type of stainless steels behind austenitics. Ferritic stainless steels with 11–30% (weight percentage) chromium have been widely used in automobiles, pressure vessels, road and rail transport, power generaion, mining [16–18], etc. FSS have been developed to fill the gap between stainless steels and the rust-prone carbon steels, thus providing an alternative that displays both the advantages of stainless steels and engineering properties of carbon steels [19,20].

Ferritic/austenitic (F/A) joints are a popular dissimilar metal combination used in many applications and these joints have huge demand in industries like petrochemical industries, ship industries, nuclear power plants, pulp and paper, [21,22], etc. F/A joints are normally produced using conventional welding processes such as manual metal arc (MMA), metal inert gas arc (MIG) and tungsten inert gas arc (TIG) welding [23]. F/A dissimilar joints are based on both technical and economical aspects i.e. these dissimilar joints can provide satisfactory performance with reasonable cost savings [24]. Satyanarayana et al. [2] mentioned that joining of ferritic stainless steels was facing problem of coarse grains in weld zone and heat affected zone of fusion weld where as austenitic stainless steels are easy weld materials. Joining of dissimilar F/A materials is not an easy task; it is considered to be a challenging problem due to differences in thermal conductivities and thermal expansion which may cause crack formation interface [25,26].

Larsson and Berthold [27] had given detailed description of both the metallurgical properties and recommended welding procedure for joining of ferritic and austenitic stainless steels. Recently; joining of dissimilar materials with use of different welding processes have received more attention for producing variety of products or parts in many industrial applications [28]. Taban et al. [19] investigated the effects of dissimilar welds between ferritic stainless steel modified 12%cr and carbon steel. Anawa and Olabi [24] optimized the tensile strength of dissimilar ferritic/austenitic metal joints in laser beam welding process. Ugur et al. [29] made an investigation on microstructural charactirstics of dissimilar AISI 430 ferritic and AISI 304 austenetic stainless steel materials. Joo et al. [30] had investigated the quality characteristics of the dissimilar welded joints between high strength steel and stainless steel in hybrid Co_2 laser GMA welding process by varying four parameters namely weld speed, welding current, laser arc distance and welding voltage. Rudrapati et al. [31] had optimized process parameters of TIG welding of dissimilar mild steel and stainless steel materials.

Palani and Murugan [32] had made an extensive analysis on significances of process parameters on quality characteristics of weldments and stated that proper selection of welding parameters were very important to eliminate/avoid weld defects and to obtain desirable weld properties in weldment. Taguchi method and grey relational analysis are efficient techniques to analyze and optimize the multi-quality characteristics in welding processes [33–36]. Pal et al. [33] had made experimental analysis to optimize multi-responses in pulsed metal inert gas welding process by using grey-based Taguchi method. The impact of individual process parameters had been identified by analysis variance. Researchers found improved welding condition(s) through hybrid gry- based Taguchi methodology. Datta et al. [34] have utilized Taguchi's OA with grey relational analysis to determine the optimal process condition for multi-responses in submerged arc welding process. Tarng et al. [35] have determined the optimal welding process parameters by using grey-based Taguchi methods in submerged arc welding process by considering multiple weld qualities. Again, Pan et al. [36] had enhanced the welding conditions to improve multiple weld qualities simultaneously with use of grey relational analysis and Taguchi method [46,47]. Again, Songsorn et al. [37] also utilized Grey–Taguchi method to predict multi-quality indices in MIG welding process.

It thus becomes obvious that welding of dissimilar materials is challenging and is not yet investigated to a fair extent. This is true in respect of welding between ferritic stainless steels and austenitic stainless steels (F/A), as well. Further, it is also important that suitability of different techniques for each combination of dissimilar materials needs to be studied thoroughly. Effect of input parameters on quality responses is always an important aspect [32]. Considering the above, the present work is planned to study the effects of input parameters on ultimate tensile strengths

Please cite this article in press as: N. Ghosh et al., GMAW dissimilar welding of AISI 409 ferritic stainless steel to AISI 316L austenitic stainless steel by using AISI 308 filler wire, Eng. Sci. Tech., Int. J. (2017), http://dx.doi.org/10.1016/j.jestch.2017.08.002

(UTS) and yield strength (YS) in GMA welding of dissimilar ferritic stainless steel AISI 409 and austenitic stainless steel AISI 316L materials. Experiments have been done as per L_9 orthogonal array of Taguchi method. Surface and sub-surface defects of weld specimens have been studied by conducting visual inspection and X-ray radiographic tests. Multi-responses: ultimate tensile strength and yield strength have been combined into one integrated quality response (grey relational grade) by using grey relational analysis. The significance of welding parameters on output responses have been studied through statistical signal-to-noise ratio technique. The optimal parametric setting for gas metal arc (GMA) welding operation for optimizing both the responses combinedly has been obtained by Taguchi method. Present work and extensive research work in this regard i.e. joining of dissimilar ferritic stainless steel AISI 409 and austenitic stainless steel AISI 316L (F/A) materials may generate sound knowledge-base from which practicing engineers and technicians may select parametric setting easily to produce good quality weld more precisely, reliably and predicatively.

2. Taguchi method

Taguchi method is developed by Dr. Genichi Taguchi, a Japanese scientist [33]. Taguchi design of experiments provides an efficient and systematic way to optimize designs for performance, quality and cost. Taguchi method is widely used in different fields of engineering to optimize the manufacturing processes/systems [38,39]. It is one of the most important tools for designing high quality systems/processes at reduced cost. Taguchi method is based on orthogonal array experiments, emphasizes balanced design with equal weightage to all factors with less number of experimental runs. Therefore, cost as well as experimental time reduced drastically with orthogonal array of Taguchi method [40]. In order to evaluate the significance of process parameters, Taguchi method uses a statistical measure of performance called signal-to-noise (S/N) ratio that takes both the mean and the variability into account [41]. The S/N ratio is the ratio of the mean (signal) to the standard deviation (noise). The ratio depends on the quality characteristics of the product/process to be optimized. The standard S/N ratios [42] generally used are nominal-is-best (NB), lower-the-better (LB) and higher-the-better (HB).

Taguchi's S/N Ratio for (NB) Nominal-the-best

$$\eta = 10 ln_{10} \frac{1}{n} \sum_{i=1}^{n} \frac{\mu^2}{\sigma^2} \tag{1}$$

Taguchi's S/N Ratio for (LB) Lower-the-better

$$\eta = -10 ln_{10} \frac{1}{n} \sum_{i=1}^{n} y_1^2 \tag{2}$$

Taguchi's S/N Ratio for (HB) Higher-the-better

$$\eta = -10 ln_{10} \frac{1}{n} \sum_{i=1}^{n} \frac{1}{y_1^2} \tag{3}$$

3. Desirability function approach

Optimization using desirability function (DF) approach is also very helpful in this context. This approach converts each of the responses (objectives) into their individual desirability value, which may vary from zero to one. If the response value is beyond the acceptable range, the desirability is assumes zero. If it reaches the target, desirability value becomes one. Corresponding to each objective, the individual desirability values are then accumulated to compute the overall or composite desirability function. The common trend is to develop a mathematical model of the composite desirability, in which it is represented as a function of process variables. Optimization is then performed to reveal factors combination to achieve maximum overall desirability.

Desirability function approach is powerful tools for solving the multiple performance characteristics optimization problems, where all the objectives are attain a definite goal simultaneously. The basic idea of this approach is to convert a multiple performance characteristics optimization problem into a single response optimization problem with the objective function of overall desirability. Then the overall desirability function is optimized. The general approach is to first convert each response y_i, into an individual desirability function d_i, that may vary over the range $0 \leq D_i \leq 1$, where if the response y_i meets the goal or target value, then $di = 1$, and if the response falls beyond the acceptable limit, then $d_i = 0$. The next step is to select the parameter combination that will maximize overall desirability D.

$$D = (d_1 \cdot d_2 \ldots d_m)^{\frac{1}{m}} \tag{4}$$

where m = number of response.

Calculate the individual desirability for the corresponding responses using the formula proposed by Derringer and Suich. There are three forms of the desirability functions according to the response characteristics.

3.1. The nominal-the-best

The value of $\hat{y}$ is required to achieve a particular target T. when the $\hat{y}$ equals to T, desirability value equals to 1; if the departure of $\hat{y}$ exceeds a particular range from the target, the desirability value equals to 0, and such situation represents the worst case. The desirability function of the nominal the best can be written as:

$$\begin{cases} \left(\frac{\hat{y}-y_{min}}{T-y_{min}}\right)^S, y_{min} \leqslant \hat{y} \leqslant T, s \geqslant 0 \\ \left(\frac{\hat{y}-y_{min}}{T-y_{min}}\right)^t, T \leqslant \hat{y} \leqslant y_{min}, t \geqslant 0 \\ 0 \end{cases} \tag{5}$$

where the ymax and ymin represent the upper and lower tolerance limits of $\hat{y}$ and s and t represent the indices.

3.2. The larger-the-better

The value of $\hat{y}$ is expected to be the larger better. When the $\hat{y}$ exceeds a particular criteria value, which can be viewed as the requirement, the desirability value equals to 1; if the $\hat{y}$ is less than a particular criteria value, which is unacceptable, the desirability equals to 0. The desirability function of the larger-the-better can be written as

$$\begin{cases} 0 & \hat{y} \leqslant y_{min} \\ \left(\frac{\hat{y}-y_{max}}{y_{max}-y_{min}}\right)^r, & y_{min} \leqslant \hat{y} \leqslant y_{max} \\ 1 & \hat{y} \geqslant y_{max} \end{cases} \tag{6}$$

3.3. The smaller-the-better

The value of $\hat{y}$ is expected to be the smaller the better. When the $\hat{y}$ is less than a particular criteria value, the desirability value equals to 1; if the $\hat{y}$ exceed a particular criteria value, the desirability value equals to 0. The desirability function of the smaller –the – better can be written as

Please cite this article in press as: N. Ghosh et al., GMAW dissimilar welding of AISI 409 ferritic stainless steel to AISI 316L austenitic stainless steel by using AISI 308 filler wire, Eng. Sci. Tech., Int. J. (2017), http://dx.doi.org/10.1016/j.jestch.2017.08.002

Table 1
Welding process parameters and their levels.

Input factors	Units	Notation	Factor levels		
			1	2	3
Welding current	**A**	A	100	112	124
Gas flow rate	l/min	B	10	15	20
Nozzle to plate distance	mm	C	9	12	15

$$\begin{cases} 1, & \hat{y} \leqslant y_{min} \\ \left(\frac{\hat{y}-y_{max}}{y_{min}-y_{max}}\right)^{r} & y_{min} \leqslant \hat{y} \leqslant y_{max}, r > 0 \\ 0, & \hat{y} \geqslant y_{min} \end{cases} \quad (7)$$

where the ymax and ymin represent the upper and lower tolerance limits of ŷ and r represent the weight .The s, t and r in Eqs. (2)(4) indicate the weight and are defined according to requirement of the user indices. If the corresponding response is expected to be closer to the target, the weight can be set to the larger value; otherwise, the weight can be set to the smaller value.

Table 2
Welding design matrix as per L_9 orthogonal array of Taguchi.

S. No	Welding parameters		
	Welding current (A)	Gas flow rate (B)	Nozzle to plate distance (C)
1	100	10	9
2	100	15	12
3	100	20	15
4	112	10	12
5	112	15	15
6	112	20	9
7	124	10	15
8	124	15	9
9	124	20	12

4. Experimental plan, set-up and procedure

Experiments have been planned as per L_9 orthogonal array of Taguchi method that is composed of three columns and nine rows. This design is selected based on three factors of three levels each. In this set of experiments, welding current, gas flow rate, and nozzle to plate distance have been considered as process variables. Welding process parameters and their levels are shown in Table 1. Welding design matrix as per L_9 Taguchi orthogonal array is shown in Table 2. Butt joints have been done between dissimilar materials: ferritic stainless steel AISI 409 and austenitic stainless steel AISI 316L, by gas metal arc (GMA) welding process by using AISI 308L austenitic filler wire. Each butt-welded sample is made by joining two 3 mm thick sheets, each of dimensions 60 mm × 100 mm × 3 mm. Welding has been carried out by ESAB-MAKE: AUTO K 400 Machine. Copper plate is used as backing plate. Welding speed is nearly kept constant 120 mm/min. Photographic view of welding set up is shown in Fig. 1. Chemical composition of austenitic stainless steel AISI 316L, ferritic stainless steel AISI 409 and filler metal are shown in Table 3. The Photographic view of the welded samples is shown in Fig. 2. And then visual inspection and X-ray radiographic test of all welded specimens have been made. After visual inspections and X-ray radiographic test, tensile test specimens have been prepared from the welded joints, by cutting/machining for conducting tensile test. During cutting/machining of the tensile test specimens, small cut- outs have been taken. These cut pieces have then been ground, polished and etched for studying microstructures. However the results of microstructure are not considered in this study. This is being considered as a separate study and critical analysis, which may come up as a separate paper.

Photographic view of tensile test specimen is shown in Fig. 3.

Fig. 1. The photographic view welding set-up.

Table 3
Chemical composition of stainless steel AISI 316L, ferritic stainless steel AISI 409 and AISI 308L austenitic filler wire.

Base plate	Composition wt%										
	C	Mn	Si	P	Cr	Ni	Mo	Cu	Al	S	T
316L	0.03	1.47	0.58	0.025	18.33	8.33	0.2	0.19	0.01	0.01	–
409	0.02	0.78	0.37	0.02	11.72	–	–	–	0.02	0.48	
Filler metal 308L	0.02	1.68	0.53	0.012	19.45	9.22	0.116	0.082	0.01	0.03	–

Please cite this article in press as: N. Ghosh et al., GMAW dissimilar welding of AISI 409 ferritic stainless steel to AISI 316L austenitic stainless steel by using AISI 308 filler wire, Eng. Sci. Tech., Int. J. (2017), http://dx.doi.org/10.1016/j.jestch.2017.08.002

Fig. 2. Photographic view of the welded sample.

5. Results of visual inspection of weldment

For visual inspection, the weld surface is observed with the naked eye, in order to detect the surface defects of the weldment. The test results of visual inspection are given in Table 4. From the Table 4, it is found that no defect is found in samples: 1, 4, 6 and 8. And welding defects such as spatter, blow holes, uneven penetrations, excessive deposition are found in other samples. The reasons for the above mentioned welding defects are discussed as follows:

1. Spatter defect as found in sample numbers: 2, 3, 5 and 9. It is caused due to damp filler rod, arc blow/bubble of gas being entrapped in the molten metal, and projecting small drops of metal outside the arc seam [43,44].
2. Welding current at too low/two high and faster travel speed or combination of both may cause blow holes in weldments, as found in sample number 2. Incorrect welding technique, unclean job surface, damp filler rod, gas getting entrapped in solidifying metal, larger arc, etc., are some of the reasons for blow holes defects in weldments [44,45].
3. Uneven penetration found in sample Nos.5 and 7, in visual inspection, may possibly be effected by wrongly held electrode/filler rod, faster arc travel speed.
4. Excessive deposition found in sample Nos. 3 and 9, in visual inspection, may possibly be effected by excess weld metal on the back side of the joint.

6. Results of X-ray radiographic tests of weldment

With the use of the XXQ-2005 X-ray flaw detector, X- ray radiographic tests have been conducted for all the 9 samples and some typical copies of radiography films of few samples are given in Figs. 4–9. Results of X-ray radiographic tests are shown in Table 5.

Fig. 4. Radiographic film for sample No.3.

Fig. 5. Radiographic film for sample No.4.

Fig. 6. Radiographic film for sample No.5.

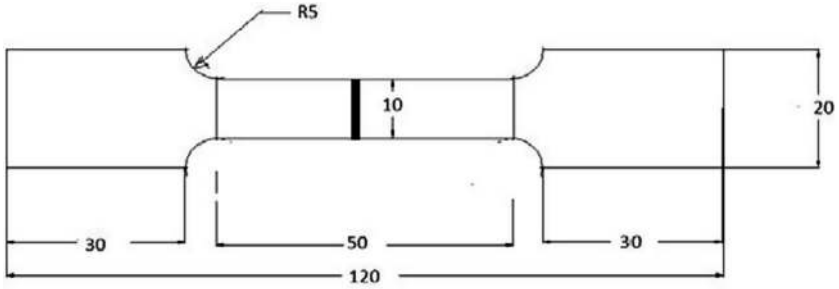

Fig. 3. Schematic diagram of the specimen prepared for tensile test as ASTM E8 standard.

Table 4
Observed results of visual inspection of weld specimens.

S. No.	Welding current (**A**)	Gas flow rate (B)	Nozzle to plate distance	Result of visual inspection
1	100	10	9	No defects
2	100	15	12	Blow hole and spatter
3	100	20	15	Excessive deposition and spatter
4	112	10	12	No defects
5	112	15	15	Spatter and uneven penetration
6	112	20	9	No defects
7	124	10	15	Uneven penetration
8	124	15	9	No defects
9	124	20	12	Spatter and excessive deposition

Please cite this article in press as: N. Ghosh et al., GMAW dissimilar welding of AISI 409 ferritic stainless steel to AISI 316L austenitic stainless steel by using AISI 308 filler wire, Eng. Sci. Tech., Int. J. (2017), http://dx.doi.org/10.1016/j.jestch.2017.08.002

Fig. 7. Radiographic film for sample No.7.

Fig. 8. Radiographic film for sample No.8.

Fig. 9. Radiographic film for sample No.9.

The lack of fusion defect is found in sample number 3. Lack of fusion at root or wall has occurred due to improper setting of the welding input parameters: current, improper cleaning, faster arc travel speed, presence of oxides, scale, etc, which do not permit the deposited metal to fuse properly with the base metal. Heat input should be optimum to prevent lack of fusion defect. Too low heat input does not ensure proper melting of the weld deposit whereas, too high heat input, makes the large weld pool, from which metal starts flow away in the area in front of the arc which prevents melting of the base metal [44].

Porosity defect has been found in sample number: 2, 5, 7 and 9 which may have resulted, due to gas being entrapped in the solidifying metal [45]. Porosity may detrimental effects on quality of weldment. The contamination of the shielding gas, filler metal and base metal may be the major problem [44]. Leaks anywhere in the distribution system allow the air to diffuse into the shielding gas. Molten weld metal holds a lot of nitrogen, oxygen and hydrogen than the base metal. As the weld puddle freezes, the gases come out of solution and form porosity. Porosity can also be caused by excessive tip-to-work distance which can create turbulence in the shielding gas column, aspirating oxygen and nitrogen from the atmosphere which then react with the high temperature weld metal. A too low or too high gas flow rate also enhances porosity. At low rates, the gas cannot exclude the atmosphere. At high flows, turbulence in the gas column causes mixing with the atmosphere.

From the results of visual inspection and X-ray radiographic tests, it is noticed that some consistency in the findings can be identified. Visual and X-ray radiographic tests also indicate that sample Nos. 1, 4, 6 and 8 has got no significant defect.

7. Tensile test results and discussion

The tensile test specimens, prepared corresponding to L_9 Taguchi Orthogonal Array design of experiments, have been tested for tensile strengths and the results obtained are given in Table 6.

8. Selection of optimum parameters using desirability function analysis

For the present work the responses should be maximized and hence larger the better formulae is used to find the individual desirability values and tabulated in Table 7 and using Eq. (4) over-

Table 6
Tensile Test result.

Sample No.	Yield strength (Mpa)	Ultimate Tensile Strength (Mpa)	Place of fracture
1	266.322	421.742	Base metal
2	280.012	407.998	HAZ
3	276.57	411.641	Base metal
4	244.719	381.214	HAZ
5	220.499	400.704	HAZ
6	230.454	345.678	HAZ
7	281.51	415.699	Base metal
8	269.953	401.790	Base metal
9	268.859	400.364	Base metal

Table 7
Individual desirability values.

Sample No.	individual desirability values	
	Yield strength (MPa)	Ultimate tensile strength (MPa)
1	0.24894	0.00000
2	0.02455	0.13603
3	0.08097	0.09997
4	0.60302	0.40112
5	1.00000	1.00000
6	0.83683	0.75283
7	0.00000	0.05981
8	0.18942	0.19747
9	0.20736	0.21158

Table 5
Results of X-ray radiographic test.

sample No.	Welding current (**A**)	Gas flow rate (B)	Nozzle to plate distance	Result of X-ray radiographic tests
1	100	10	9	No defects
2	100	15	12	Porosity
3	100	20	15	Lack of fusion and porosity
4	112	10	12	No defects
5	112	15	15	Porosity
6	112	20	9	No defects
7	124	10	15	Porosity
8	124	15	9	No defects
9	124	20	12	Porosity

Please cite this article in press as: N. Ghosh et al., GMAW dissimilar welding of AISI 409 ferritic stainless steel to AISI 316L austenitic stainless steel by using AISI 308 filler wire, Eng. Sci. Tech., Int. J. (2017), http://dx.doi.org/10.1016/j.jestch.2017.08.002

Table 8
overall desirability values.

Sample No.	overall desirability
1	0.00000
2	0.05778
3	0.08997
4	0.49182
5	1.00000
6	0.79375
7	0.00000
8	0.19340
9	0.20946

Table 9
Response table for overall desirability.

Level	current	Gas flow rate	Nozzle To Plate Distance
1	0.04925	0.16394	0.32905
2	**0.76186**	**0.41706**	0.25302
3	0.13429	0.36439	**0.36332**
Delta	0.71261	0.25312	0.1103
Rank	1	2	3

all desirability values are calculated and tabulated in the Table 8 (See Table 9).

With the help of Response graph for mean grey relational grade (Fig. 10) optimum parametric combination has been determined. The optimal factor setting becomes **C2F2S3** (i.e. welding current = 112 A, Gas flow rate = 15 *l*/min and Nozzle to plate distance = 15 mm

9. Results of confirmatory test

The results of confirmatory test are shown in Table 10. It is found that prediction of optimal parameter setting is valid.

Table 10
Confirmatory results.

Obtained optimum parametric condition by Taguchi method		Obtained ultimate Tensile strength (U.T.S) by confirmatory test
Current (C)	112 A	
Glass flow rate (F)	15 L/min	U.T.S = 422 MPa
Nozzle to plate distance (S)	15 mm	

Confirmatory test is conducted at optimal parameter combination (C2F2S3) to check the validity of the optimum welding condition. From the results of confirmatory test, it is found that optimum welding parametric condition produced maximum UTS, this value shows the validation of the proposed optimization methodology

10. Conclusions

Following conclusions are drawn in respect of MIG welding of AISI 409 Ferritic Stainless steel to AISI 316L austenitic stainless steel.

- The best result is obtained for the sample No.1 (Corresponding to current 100 A, flow rate 10 L/min and Nozzle to plate distance 9 mm) For this sample, ultimate tensile strength = 421.742 MPa and Yield strength = 266.322 MPa. The worst result in tensile testing has been obtained for the sample No. 6 (corresponding to current 112 A, gas flow rate 20 L/min and nozzle to plate distance 9 mm) for this sample yield strength 230.454 MPa and Ultimate tensile strength 345.678 MPa.
- Optimization of the process parameters has been done by using Taguchi-Desirability analysis; optimum parametric combination has been determined. The optimal factor setting becomes **C2F2S3** (i.e. welding current = 112 A, Gas flow rate = 15 *l*/min and Nozzle to plate distance = 15 mm.

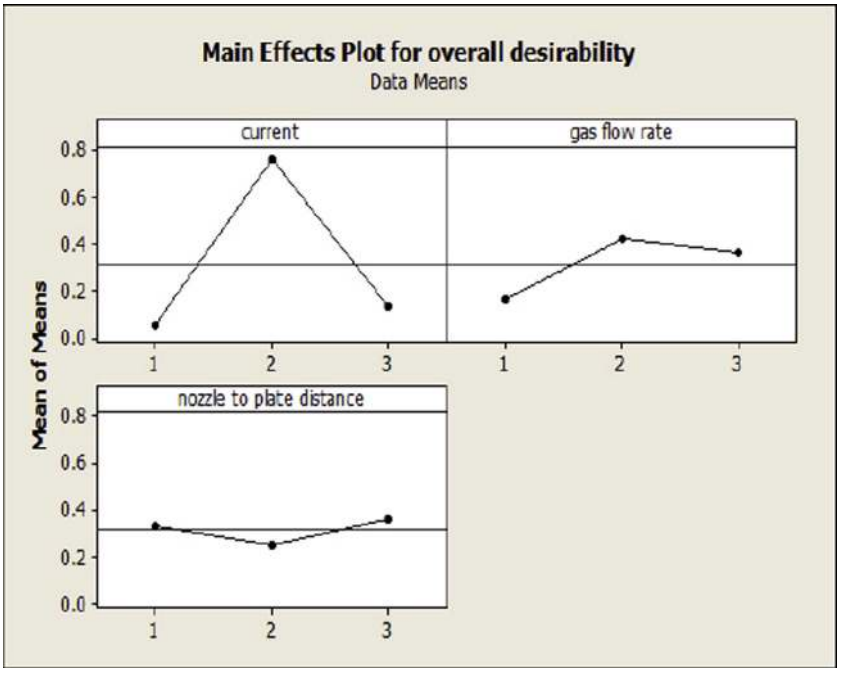

Fig. 10. Response graph for mean overall desirability.

Please cite this article in press as: N. Ghosh et al., GMAW dissimilar welding of AISI 409 ferritic stainless steel to AISI 316L austenitic stainless steel by using AISI 308 filler wire, Eng. Sci. Tech., Int. J. (2017), http://dx.doi.org/10.1016/j.jestch.2017.08.002

Acknowledgements

The authors sincerely thanks all the staff members of Blue Earth workshop of Jadavpur University who directly or indirectly made their involvement in the experimental work and testing part of this work.

References

[1] C. Rakesh, P. Riddhish, I. Asha, Reliability of dissimilar metal joints using fusion welding: a review, in: Int. Conf. on Machine Learning, Electrical and Mecha. Engi. Dubai, 2014.
[2] V.V. Satyanarayana, G.M. Reddy, T. Mohandas, Dissimilar metal friction welding of austenitic–ferritic stainless steels, J. Mater. Process. Technol. 160 (2005) 128–137.
[3] C. Augustine, B.P. George, R. Sudhish, Parametric optimization of GMAW of dissimilar steels: duplex stainless steel 2205 and stainless steel 316L, in: Int. J. on Theor. and Appl. Resea. in Mech. Engi. 3, 2014, pp. 2319–3182.
[4] I.Z. Ibrahim, S.A. Mohamat, A. Amir, A. Ghalib, The effect of gas metal arc welding processes on different welding parameters, Procedia Eng. 41 (2012) 1502–1506.
[5] M. Singla, D. Singh, D. Deepak, Parametric optimization of gas metal arc welding processes by using factorial design approach, J. Miner. Mater. Charact. Eng. 9 (2010) 353–363.
[6] U. Esme, M. Bayramoglu, Y. Kazancoglu, S. Ozgun, Optimization of weld bead geometry in TIG Welding process using grey relation analysis and Taguchi method, Mater. Technol. 43 (2009) 143–149.
[7] S. Datta, G. Nandi, A. Bandyopadhyay, P.K. Pal, Application of PCA-based hybrid Taguchi method for correlated multicriteria optimization of submerged arc weld: a case study, Int. J. Adv. Manuf. Technol. 45 (2009) 276–286.
[8] N. Ghosh, P.K. Pal, G. Nandi, R. Rudrapati, Experimental investigation of TIG welding of austenitic stainless steel with change in composition of filler material, in: Proceedings of the National Conf. on Recent Trends in Manuf. Science and Technol. Kolkata, 2013, pp. 27–35.
[9] B. Weiss, R. Stickler, Phase instabilities during high temperature exposure of 316 austenitic stainless steel, Metall. Trans. 3 (1972) 851–866.
[10] C. Balaji, S.V.A. Kumar, S.A. Kumar, R. Satish, Evaluation of mechanical properties of SS 316 L weldments using tungsten inert gas welding, Int. J. Eng. Sci. Technol. 4 (2012) 2053–2057.
[11] P. Bharath, V.G. Sridhar, M. Senthilkumar, Optimization of 316 stainless steel weld joint characteristics using Taguchi technique, Procedia Eng. 97 (2014) 881–891.
[12] G.J. Parr, A. Handson, Introduction to Stainless Steel, American Society for Metals, USA, 1963.
[13] J.A. Sedriks, Corrosion of Stainless Steels, Wiley, New York, 1996.
[14] R.M. Molak, K. Paradowski, T. Brynk, L. Ciupinski, Z. Pakiela, K.J. Kurzydlowski, Measurement of mechanical properties in a 316L stainless steel welded joint, Int. J. Pressure Vessels Piping 86 (2009) 43–47.
[15] P. Sathiya, S. Aravindan, A.N. Haq, Effect of friction welding parameters on mechanical and metallurgical properties of ferritic stainless steel, Int. J. Adv. Manuf. Technol. 31 (2007) 1076–1082.
[16] H. Shengsun, H. Ruifeng, S. Jungi, H. Jian, X. Haigang, Effect of pulse frequency on microstructure of 21% Cr ferritic stainless steel in pulsed gas tungsten arc welding, Trans. Tianjin Univ. 19 (2013) 127–129.
[17] D. Qizhan, Welding of Stainless Steel [M], China Machine Press, China, 2009.
[18] S. Afshan, L. Gardner, Experimental study of cold-formed ferritic stainless steel hollow sections, J. Struct. Eng. 139 (2013) 717–728.
[19] E. Taban, E. Deleu, A. Dhooge, E. Kaluc, Evaluation of dissimilar welds between ferritic stainless steel modified 12% Cr and carbon steel S355, Weld. J. 87 (2008) 291s–297s.
[20] M. Li, H. Shengsun, H. Bao, S. Junqi, W. Yonghui, Activating flux design for laser welding of ferritic stainless steel, Trans. Tianjin Univ. 20 (2014) 429–434.
[21] M. Arivarasu, D.R. Kasinath, A. Natarajan, Effect of continuous and pulsed current on the metallurgical and mechanical properties of gas tungsten arc welded AISI 4340 aeronautical and AISI 304 L austenitic stainless steel dissimilar joints, Mater. Res. 18 (2015) 59–77.
[22] J.N. Dupont, C.S. Kusko, Technical note: Martensite formation in austenitic/ferritic dissimilar alloy welds, Weld. J. (2007) 51–54.
[23] Z. Sun, Feasibility of producing ferritic/austenitic dissimilar metal joints by high energy density laser beam process, Int. J. Pressure Vessel Piping. 68 (1996) 153–160.
[24] E.M. Anawa, A.G. Olabi, Optimization of tensile strength of ferritic/austenitic laser-welded components, Opt. Lasers Eng. 46 (2008) 571–577.
[25] S. Allabhakshi, M.G. Reddy, V.V. Ramarao, P.C. Babu, C.S. Ramachandran, Studies on weld overlaying of austenitic stainless steel (AISI 304) with ferritic stainless steel (AISI 430), in: Proceedings of the National Welding Conf. Chennai, 2002.
[26] A. Omar, Effects of welding parameters on hard zone formation at dissimilar metal welds, Weld. J. 77 (1998) 86s–93s.
[27] B. Larsson, L. Berthold, Fabrication of ferritic – austenitic stainless steels, Mater. Des. 7 (1986) 81–88.
[28] A. Thomas, Gas shielded arc welding of ferrite-austenetic steels, Weld. Int. 24 (2010) 861–866.
[29] C. Ugur, D. Halil, T. Mustafa, Microstructural characteristic of dissimilar welded components (AISI ferritic – AISI 304 austenetic stainless steels) by CO2 laser beam welding, GU J. Sci 25 (2012) 35–51.
[30] S.M. Joo, H.S. Bang, S.Y. Kwak, Optimization of hybrid CO2 laser-GMA welding parameters on dissimilar materials AH32/STS304L using grey-based Taguchi analysis, Int. J. Precis. Eng. Manuf. 15 (2014) 447–454.
[31] R. Rudrapati, N. Choudhury, A. Bandyopadhyay, Parametric optimization of TIG welding process in butt joining of mild steel and stainless steel, Int. J. Curr. Eng. Technol. (2016) 144–149.
[32] P.K. Palani, N. Murugan, Selection of process parameters of pulsed current gas metal arc welding, J. Mater. Process. Technol. 172 (2006) 1–10.
[33] S. Pal, S.K. Malviya, S.K. Pal, A.K. Samantaray, Optimization of quality characteristics parameters in a pulsed metal inert gas welding process using grey-based Taguchi method, Int. J. Adv. Manuf. Technol. 44 (2009) 1250–1260.
[34] S. Datta, A. Bandyopadhyay, P.K. Pal, Grey-based taguchi method for optimization of bead geometry in submerged arc beadon-plate welding, Int. J. Adv. Manuf. Technol. 39 (2007) 1136–1143.
[35] Y.S. Tarng, S.C. Juang, C.H. Chang, The use of grey-based Taguchi methods to determine submerged arc welding process parameters in hardfacing, J. Mater. Process. Technol. 128 (2002) 1–6.
[36] L.K. Pan, C.C. Wang, S.L. Wei, H.F. Sher, Optimizing multiple quality characteristics via Taguchi method-based Grey analysis, J. Mater. Process. Technol. 182 (2007) 107–116.
[37] K. Songsorn, K. Sriprateep, S. Rittidech, Grey-Taguchi method to optimize the percent zinc coating balances edge joints for galvanized steel sheets using metal inert gas pulse brazing process, Adv. Mech. Eng. 8 (2016) 1–14.
[38] R.K. Roy, Design of Experiments Using the Taguchi Approach, Wiley, New York, 2001.
[39] S. Vinodh, S.K. Bharathi, N. Gopi, Parametric optimization of submerged arc welding using Taguchi method, Des. Exp. Prod. Eng. (2016) 183–196.
[40] Y.S. Tarng, W.H. Yang, Optimisation of the weld bead geometry in gas tungsten arc welding by the Taguchi method, Int. J. Adv. Manuf. Technol. 14 (1998) 549–554.
[41] A.K. Singh, D. Tapas, V. Dey, R.N. Rai, An approach to maximize weld penetration during TIG welding of P91 steel plates by utilizing image processing and Taguchi orthogonal array, J. Inst. Eng. India Ser. C (2016), http://dx.doi.org/10.1007/s40032-016-0268-3.
[42] S.V. Sapakal, M.T. Telsang, Parametric optimization of MIG welding using Taguchi design method, Int. J. Adv. Eng. Res. Stud. 1 (2012) 28–30.
[43] A.C. Davies, The Science and Practice of Welding vol. 2, Cambridge University Press, Cambridge, 1992.
[44] N. Ghosh, P.K. Pal, G. Nandi, Parametric optimization of MIG welding on 316L austenitic stainless steel by grey based Taguchi method, Procedia Technol. 25 (2016) 1038–1048.
[45] P.N. Rao, Manufacturing Technology Volume-1, Tata Mc Graw –Hill Publishing Company Limited, New Delhi, 2009.
[46] N. Choudhury, R. Rudrapati, A. Bandyopadhyay, Design optimization of process parameters for TIG welding based on Taguchi method, Int. J. Curr. Eng. Technol. (2014) 12–16.
[47] N. Kumar, R. Rudrapati, P.K. Pal, Multi-objective optimization in through laser transmission welding of thermoplastics using grey based Taguchi method, Procedia Mater. Sci. 5 (2014) 2178–2187.

Please cite this article in press as: N. Ghosh et al., GMAW dissimilar welding of AISI 409 ferritic stainless steel to AISI 316L austenitic stainless steel by using AISI 308 filler wire, Eng. Sci. Tech., Int. J. (2017), http://dx.doi.org/10.1016/j.jestch.2017.08.002